Journal of Porphyrins and Phthalocyanines
J. Porphyrins Phthalocyanines 2020; **24**: 1083–1092
DOI: 10.1142/S1088424620500297

Published at https://www.worldscinet.com/jpp/

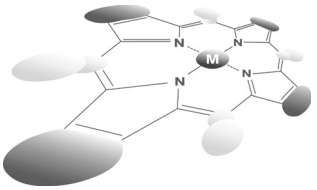

Tetra-(benzo-24-crown-8)-phthalocyanines as a platform for supramolecular ensembles: Synthesis and interaction with viologen

Evgeniya A. Safonova[a], Jennifer A. Wytko*[b◊], Jean Weiss[b◊], Elena A. Ugolkova[c], Nikolay N. Efimov[c], Vadim V. Minin[c], Yulia G. Gorbunova*[a,c◊] and Aslan Yu. Tsivadze[a,c]

[a]*A.N. Frumkin Institute of Physical Chemistry and Electrochemistry RAS, 119071, Leninsky pr., 31, building 4, Moscow, Russia*
[b]*Institut de Chimie de Strasbourg, UMR 7177, CNRS, Université de Strasbourg, 4 Rue Blaise Pascal, 67008 Strasbourg, France*
[c]*N.S. Kurnakov Institute of General and Inorganic Chemistry RAS, 119991, Leninsky pr., 31, Moscow, Russia*

Received 4 May 2020
Accepted 18 June 2020

ABSTRACT: The synthesis of a series of novel tetra-(benzo-24-crown-8)-phthalocyanines (Mg(II), Ni(II) and Co(II)) as well as a modified procedure for the free-base ligand and its Zn(II) and Cu(II) complexes are reported. The tendency of these phthalocyanines to undergo supramolecular cofacial dimerization induced by interaction with a viologen (*N,N*-di(but-3-ynyl)-4,4′-bipyridinium) was investigated by UV-vis absorption and EPR spectral studies in solution. The nature of the metal cation in phthalocyanine, the concentration, as well as the solvent all influenced the assembly processes.

KEYWORDS: phthalocyanine, crown ether, viologen, supramolecular assembly, UV-vis absorption, EPR spectroscopy.

INTRODUCTION

The development of molecular machines and switches is on the foremost edge of today's science [1–5]. Applications of such molecular devices include multiple aspects of modern life [6], medicine [7, 8] and electronics [9, 10], as well as artificial small-molecule robots [11]. Conceptually, it should be possible to develop materials for information recording and storage with unique density, where one molecule bears one information bit, or for the control of drug delivery with target carriers. Tetrapyrrolic macrocycles are very promising scaffolds for the formation of molecular machines and switches because of their chemical and thermal stability along with their intense absorbance in the UV and visible spectral range and remarkable photochemical and redox properties [4, 12, 13].

Initially designed for the recognition of alkali and alkaline-earth metal ions, crown ethers have shown strong affinities for ammonium- and pyridinium-based organic cations and thus have also often been used for molecular machine development [14–17]. Crown-substituted tetrapyrrolic macrocycles [18–20] that integrate the features of both classes of substances may be interesting platforms for the construction of novel molecular machines. For example, tetra-(benzo-24-crown-8)-phthalocyanine has been used as a versatile building block for the design of a fourfold rotaxane consisting of cofacially stacked homo- or heteronuclear phthalocyanine (Pc)–porphyrin (Por) dimers [21–24]. Switchable spin–spin interactions in such rotaxanes have been induced by supramolecular interactions between crown ethers appended to phthalocyanines and protonated amino groups of a neighboring porphyrin molecule. More complex trinuclear porphyrin-Pc

[◊] SPP full member in good standing.

*Correspondence to: Jennifer Wytko, email: jwytko@unistra.fr, Yulia Gorbunova, email: yulia@igic.ras.ru.

assemblies have been designed by three approaches. The first strategy was the introduction of additional porphyrin molecules as the third deck in the rotaxane structure using specific recognition due to ionic interactions [25]. The second approach involved the assembly of two phthalocyanine molecules onto a porphyrin template containing eight amino-groups to form a heterotrimer H_2Por-Cu(II)Pc-Cu(II)Pc [26]. The last approach was the design and synthesis of another type of triple-decker assembly, namely a multiply interlocked catenane with a novel molecular topology, in which four peripheral crown ethers were quadruply interlocked with a cofacial porphyrin dimer bridged with four alkylammonium chains [27].

Today, no examples of scaffolds built on phthalocyanines have been reported in the literature. This work reports the design of a new type of molecular device based on tetra-(benzo-24-crown-8)-phthalocyanine **8M** in which the crown ether ring could bind positively charged viologens to form cofacial dimers (Fig. 1). Since viologens can exist in three distinct redox states, the electrochemical control of the dynamic states could be used for the further design of a device constructed on the basis of such supramolecular assemblies [28–30]. The ethynyl groups of the viologens offer the future possibility of locking the dimeric structure by a click reaction with bulky azide stoppers. In this work, the synthesis of tetra-(benzo-24-crown-8)-substituted phthalocyanine and its metal complexes **8M** (Mg(II), Ni(II), Co(II)), Zn(II) and Cu(II)) as well as their supramolecular interactions with a viologen (*N,N*-dibutynyl-4,4′-bipyridinium) are described. The formation of supramolecular cofacial dimers in solution is investigated in detail by UV-vis and EPR spectroscopy.

EXPERIMENTAL

Materials and equipment

Triethyleneglycol monotosylate (**2**), 1,2-bis-2′-[2″-(2‴-hydroxyethoxy)-ethoxy]-ethoxy}-benzene (**3**) and 1,1′-di(but-3-ynyl)-4,4′-bipyridine-1,1′-diium bis(hexafluorophosphate (**9**) were synthesized by previously reported procedures [31–33].

Triethyleneglycol (**1**), *p*-toluenesulphonylchloride (TsCl), NaOH, K_2CO_3, catechol, *N*-bromosuccinimide (NBS), I_2, imidazole, triphenylphosphine (PPh_3), Cs_2CO_3, $Zn(CN)_2$, $Pd_2(dba)_3$, dppf, $Cu(OAc)_2$, $Zn(OAc)_2 \cdot 2H_2O$ $Mg(OAc)_2 \cdot H_2O$, Mg, $Co(OAc)_2 \cdot 4H_2O$, $Ni(acac)_2$, CF_3COOH, 1,8-diazabicyclo[5.4.0]-undec-7-ene (DBU) and the solvents (tetrahydrofuran (THF), *N,N*-dimethylformamide (DMF), *N,N*-dimethylacetamide (DMA), pentanol, dichlorobenzene, dichloromethane, chloroform, ethanol and methanol) were acquired from commercial suppliers (Acros, Merck, Aldrich, and Sigma). Pentanol was distilled over magnesium under argon. DBU was distilled over CaH_2 under reduced pressure, and stored under argon. Chloroform (stabilized with 0.6–1% ethanol) was dried over $CaCl_2$ and distilled over $NaHCO_3$. Other reagents were used without additional purification. Neutral alumina (Merck) and silica gel (Macherey Nagel, Kieselgel 60) were used for column chromatography. Bio-Beads SX-1 (BIO-RAD) were used for size-exclusion chromatography.

NMR spectra were recorded on Bruker Avance 600 and Bruker Avance 300 spectrometers. NMR spectra were referenced to the residual solvent signals [27]. UV-vis spectra were measured with a Thermo Evolution 210 spectrometer in quartz cells with a 1 cm and 0.1 cm optical path equipped with a Peltier thermostating accessory.

Matrix-assisted laser desorption ionization time-of-flight mass spectra (MALDI-TOF MS) were measured on a Bruker Daltonics Ultraflex spectrometer with 2,5-dihydroxybenzoic acid as the matrix. High-resolution mass spectrometry (HRMS) experiments were performed on a Bruker Daltonics microTOF spectrometer (Bruker Daltonik GmgH, Bremen, Germany) by the Service de Spectrométrie de Masse de la Fédération de Chimie "Le Bel" (FR 2010). X-Band EPR spectra were measured at a 9.8 GHz microwave frequency on a Bruker Elexsys E-680X radiospectrometer at 90 K. Resulting EPR spectra of **8Co** and **8Cu** were described using rhombic spin Hamiltonian with Zeeman, hyperfine and super hyperfine interactions (Equation 1).

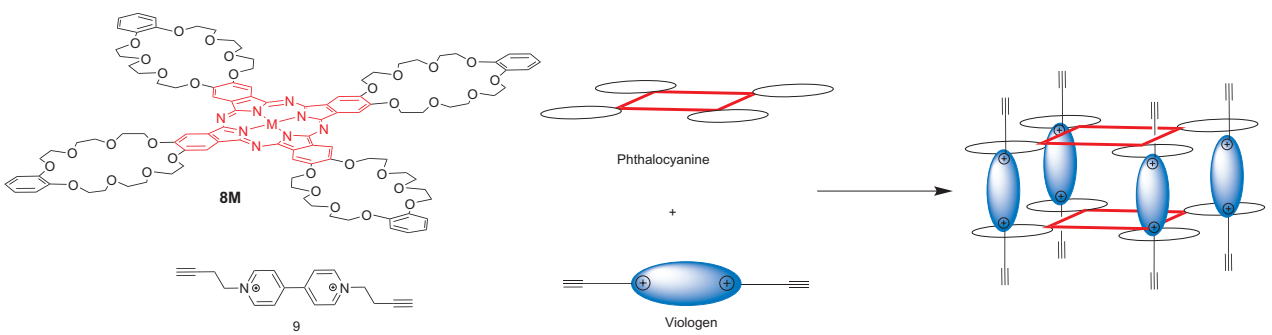

Fig. 1. Viologen-induced formation of cofacial dimers of **8M**.

$$H = g_z\beta H_z S_z + g_x\beta H_x S_x + g_y\beta H_y S_y + AI_z S_z + BI_x S_x + CI_y S_y + \beta\sum_{\alpha}(g_z a_z^{\alpha} S_z I_z^{\alpha} + g_x a_x^{\alpha} S_x I_x^{\alpha} + g_y a_y^{\alpha} S_y I_y^{\alpha}) \quad (1)$$

Here g_z, g_x, $g_y - z, x, y$ are components of the g-tensor, $A, B, C–z, x, y$ are components of the HFS tensor, S_z, S_x and S_y are projections of the spin operator onto coordination axes, $S = 1/2$, I_z, I_x and I_y are projections of nuclear spin operators onto coordination axes, $I_{Cu} = 3/2$, $I_{Co} = 7/2$. $I^i = 1$ is the nuclear spin of nitrogen and a_z, a_x and a_y are components of super hyperfine tensors in Gauss.

The resulting EPR spectrum of **8Cu** + **viologen** is the sum of the dimer spectrum with $S = 1$ and the monomer spectrum with $S = 1/2$ and was described using spin Hamiltonian with fine interactions for $S = 1$ (Equation 2).

$$H = \beta(g_x S_x H_x + g_y S_y H_y + g_z H_z S_z) + D(S_z^2 - S(S+1)/3) \quad (2)$$

Where D is the component of the fine interaction tensor.

The parameters of EPR spectra were found using the best approximation method, which minimizes the error function (Equation 3).

$$F = \sum_i (Y_i^T - Y_i^E)^2 / N \quad (3)$$

Here Y_i^E is the array of the observed intensities of EPR signals at different values of magnetic field H, Y_i^T represents the theoretical values of intensities at the same values of magnetic field H and N indicates the number of points.

Theoretical spectra were plotted according to a previously reported procedure [34]. Line shapes were described using Gaussian and Lorentzian functions [35]. The line widths were parameterized using relaxation theory [36] (Equation 4).

$$\sigma_k = \alpha_k + \beta_k m_I + \gamma_k m_I^2 \quad (4)$$

Here m_I is the projection of nuclear spin on the magnetic field direction and $k = x, y, z$, α_k, β_k, γ_k represent broadening parameters in corresponding orientations. Minimization of error function implied variation of g-factors, HFS and super hyperfine constants, line widths and shapes.

Synthesis

***Preparation of* 4,5-*bis*-2′-[2″-(2‴-*hydroxyethoxy*)-*ethoxy*]-*ethoxy*}-1,2-*dibromobenzene* (4).** A solution of NBS (2.29 g, 16.4 mmol) in 20 mL of DMF was added to a solution of **3** (2.19 g, 7.5 mmol) in 20 mL of DMF. The reaction mixture was stirred for 3 days open to air at room temperature. A saturated aqueous solution of Na_2SO_3 was added. The reaction mixture was filtered and the solvent was evaporated from the filtrate. The resulting compound was purified by chromatography on silica by gradient elution with a mixture of hexane-CH_2Cl_2–EtOH (1:1:0–0:95:5), yielding 2.67 g of **4** as a yellowish oil (86%). ^{1}H NMR (600 MHz, $CDCl_3$) δ 7.15 (s, 1H, H_{Ar}), 4.15–4.18 (m, 2H, a_1), 3.84–3.93 (m, 2H, a_2), 3.73–3.77 (m, 4H, a_3,a_4), 3.68–3.72 (m, 2H, a_5), 3.62–3.64 (m, 2H, a_6).

***Preparation of* 4,5-*bis*-2′-[2″-(2‴-*iodoethoxy*)-*ethoxy*]-*ethoxy*}-1,2-*dibromobenzene* (5).** PPh_3 (2.33 g, 9.1 mmol) and I_2 (2.22 g, 8.7 mmol) were dissolved in 85 mL of CH_2Cl_2 (freshly distilled over $CaCl_2$) and then imidazole (1.16 g, 17.0 mmol) was added. The mixture was stirred for 10 min and then **1** (0.968 g, 18.2 mmol) was added. The reaction mixture was stirred for 2 h at room temperature, then a solution of Na_2SO_3 (0.97 g, 7.7 mmol) in 15 mL of water was added. The organic layer was separated and the solvent was evaporated. The resulting compound was purified by column chromatography on silica by gradient elution with a mixture of hexane-CH_2Cl_2-EtOH (1:1:0–0:95:5) to afford 0.84 g of **5** as a yellow oil (61%). ^{1}H NMR (600 MHz, $CDCl_3$) δ, ppm: 7.15 (s, 1H, H_{Ar}), 4.14 (t, $J = 4.9$ Hz, 2H, a_1), 3.86 (t, $J = 4.9$ Hz, 2H, a_2), 3.76 (t, $J = 6.8$ Hz, 2H, a_3), 3.72 (m, 2H, a_4), 3.68 (m, 2H, a_5), 3.26 (t, $J = 6.8$ Hz, 2H, a_6). ^{13}C-NMR (151 MHz, $CDCl_3$) δ, ppm: 149.0, 119.4, 115.6, 72.2, 71.1, 70.5, 69.9, 69.5, 3.1. HRMS ESI: m/z calculated for $C_{18}H_{26}Br_2I_2O_6$ $[M + NH_4]^+$ – 769.8504, m/z found $[M + NH_4]^+$ – 769.8511; m/z calculated for $[M + Na]^+$ – 774.8058, m/z found $[M + Na]^+$ – 774.8079; m/z found for $C_{18}H_{26}Br_2I_2O_6$ $[M + K]^+$ – 790.7798, m/z found $[M + K]^+$ – 790.7799.

***Preparation of* 4′,5′-*dibromodibenzo*-24-*crown*-8-*ether* (6).** A solution of **5** (1.20 g, 1.6 mmol) and catechol (0.17 g, 1.6 mmol) in 10 mL of DMF was added by syringe pump over 10 h to a suspension of Cs_2CO_3 (2.60 g, 8.0 mmol) in 50 mL of DMF at 80 °C in argon. Then reaction mixture was stirred for 2 h and cooled to room temperature. The resulting mixture was filtered and the solvent was evaporated from the filtrate. The resulting compound was purified by chromatography on silica in a mixture of CH_2Cl_2–EtOH (95:5) to yield 0.52 g of **6** as a colorless solid (54%). M.p. = 101–104 °C. ^{1}H NMR (600 MHz, $CDCl_3$) δ, ppm: 7.06 (s, 1H, α-H_{Ar}), 6.85–6.91 (m, 2H, β,γ-H_{Ar}), 4.13–4.16 (m, 2H, CH_2), 4.09–4.11 (m, 2H, CH_2), 3.87–3.92 (m, 4H, CH_2), 3.81 (dd, $J = 6.5$, 2.0 Hz, 4H, CH_2). ^{13}C-NMR (151 MHz, $CDCl_3$) δ, ppm: 149.1, 149.0, 121.6, 118.6, 115.4, 114.3, 71.5, 71.4, 70.1, 70.0, 69.8, 69.5.

***Preparation of* 8′,9′-*benzo*-24-*crown*-8-*phthalonitrile* (7).** To a degassed mixture of **6** (270 mg, 450 μmol), $Zn(CN)_2$ (84 mg, 710 μmol), $Pd_2(dba)_3$ (20 mg, 30 μmol) and dppf (21 mg, 37 μmol), 4 mL of DMA were added. The mixture was refluxed for 2 h, cooled to room temperature, diluted with CH_2Cl_2 and filtered over a pad of alumina.

The solvent was evaporated and the resulting product was purified by column chromatography on alumina (CH_2Cl_2–EtOH (95:5)) to yield 0.204 mg of **7** as a brownish solid (91%). M.p. = 104–107 °C. ^{1}H NMR (600 MHz, $CDCl_3$) δ, ppm: 7.11 (s, 1H, α-H_{Ar}), 6.83–6.92 (m, 2H, β,γ-H_{Ar}), 4.17–4.23(m, 2H, CH_2), 4.10–4.16 (m, 2H, CH_2), 3.87–3.97 (m, 4H, CH_2), 3.81 (s, 4H, CH_2). ^{13}C-NMR (151 MHz, $CDCl_3$) δ, ppm: 152.5, 149.0, 121.7, 116.5, 115.8, 114.2, 109.1, 71.7, 71.4, 70.7, 70.2, 70.1, 69.4.

***Preparation of Mg*[(B24C8)$_4$*Pc*] (8*Mg*). *Method* 1.** A mixture of phthalonitrile **7** (200 mg, 402 μmol), $Mg(OAc)_2$ (28 mg, 201 μmol) and DBU (60 μl, 400 μmol) in 5 mL of pentanol was refluxed overnight under argon. The reaction mixture was cooled to room temperature and poured into hexane. The resulting precipitate was filtered, washed with hexane and dissolved in $CHCl_3$. The solvent was evaporated under vacuum. The product was purified by size-exclusion chromatography on a column packed with Bio-Beads SX-1 in $CHCl_3$ + 2.5 vol % MeOH yielding 80 mg of green solid (39%).

***Method* 2.** A mixture of phthalonitrile **7** (200 mg, 402 μmol), and metallic Mg (19 mg, 804 μmol) in 10 mL of pentanol was refluxed overnight under argon. The reaction mixture was cooled to room temperature and poured into hexane. The resulting precipitate was filtered, washed with hexane and dissolved in $CHCl_3$. The solvent was evaporated under vacuum. The product was purified by size-exclusion chromatography with Bio-Beads SX-1 in $CHCl_3$ + 2.5 vol % MeOH to yield 130 mg of **8Mg** as a green solid (64%). HRMS ESI, m/z: calculated for $C_{104}H_{120}MgN_8O_{32}$ — 2017, 7884, found — 2017.7847. ^{1}H NMR (600 MHz, $CDCl_3$) δ, ppm: 8.93 (s, 1H, α-H_{Ar}), 6.78–6.85 (m, 2H, β,γ-H_{Ar}), 4.67–4.73 (bs, 2H, CH_2), 3.72–4.23 (m, 10H, CH_2). UV-vis ($CHCl_3$), λ, nm (log(ε))*:* 678 (5.30), 613 (4.53), 360 (4.92), 283 (5.08).

***Preparation of H$_2$*[(B24C8)$_4$*Pc*] (8*H2*).** CF_3COOH (0.5 mL, 650 μmol) was added to a solution of **8Mg** (77 mg, 38 μmol) in 12 mL of $CHCl_3$ and the reaction mixture was refluxed for 10 min. The mixture was cooled to room temperature and neutralized with Et_3N (1 mL, 650 μmol). Solvents were removed under vacuum. The resulting product was dissolved in $CHCl_3$ and washed with water. The organic layer was dried with Na_2SO_4 and the solvent was evaporated. Column chromatography over alumina in a CH_2Cl_2/MeOH mixture (95:5) afforded a green compound, which was further purified by repetitive size-exclusion chromatography (Bio-Beads SX-1 in $CHCl_3$ + 2.5 vol % MeOH). Yield: 63 mg (80%). MALDI-TOF MS, m/z: calculated for $C_{104}H_{122}N_8O_{32}$ — 1995.82, found — 1995.8. ^{1}H NMR (600 MHz, $CDCl_3$) δ, ppm: 8.58 (s, 1H, α-H_{Ar}), 6.77–6.86 (m, 2H, β,γ-H_{Ar}), 4.72–4.77 (bs, 2H, CH_2), 4.23–4.33 (m, 2H, CH_2), 4.15–4.21 (m, 2H, CH_2), 4.05–4.09 (m, 2H, CH_2), 3.96–4.02 (m, 4H, CH_2). UV-vis ($CHCl_3$), λ, nm (log(ε))*:* 701 (5.10), 663 (5.02), 602 (4.39), 420 (4.56), 348 (4.90), 294 (4.75).

***Preparation of Zn*[(B24C8)$_4$*Pc*] (8*Zn*).** A mixture of phthalonitrile **7** (100 mg, 200 μmol), and $Zn(OAc)_2 \cdot 2H_2O$ (19 mg, 100 μmol) in 7 mL of pentanol was heated to reflux and then DBU (30 μl, 200 μmol) was added. The reaction mixture was refluxed overnight under argon, then cooled to room temperature and poured into hexane. The resulting precipitate was filtered, washed with hexane and dissolved in $CHCl_3$. Solvent was evaporated under vacuum. The product was purified by size-exclusion chromatography (Bio-Beads SX-1 in $CHCl_3$ + 2.5 vol % MeOH) to yield 90 mg of **8Zn** as a green solid (87%). HRMS ESI, calculated for $C_{104}H_{120}ZnN_8O_{32}$ — 2058.7317, found — 2058.7306. ^{1}H NMR (300 MHz, $CDCl_3$) δ, ppm: 8.87 (s, 1H, α-H_{Ar}), 6.79–6.88 (m, 2H, β,γ-H_{Ar}), 4.74 (bs, 2H, CH_2), 4.16–4.24 (m, 4H, CH_2), 4.01–4.06 (m, 2H, CH_2), 3.92–4.00 (m, 4H, CH_2). UV-vis ($CHCl_3$), λ, nm (log(ε))*:* 680 (5.14), 614 (4.71), 358 (4.24).

***Preparation of Ni*[(B24C8)$_4$*Pc*] (8*Ni*).** A mixture of **8H2** (50 mg, 25 μmol) and $Ni(acac)_2$ (13 mg, 50 μmol) in 10 mL of dichlorobenzene was refluxed for 15 min under argon. The reaction mixture was cooled to room temperature and poured into hexane. The resulting precipitate was filtered, washed with hexane and dissolved in $CHCl_3$. The solvent was evaporated under vacuum. The product was purified by size-exclusion chromatography (Bio-Beads SX-1 in $CHCl_3$ + 2.5 vol % MeOH) to yield 42 mg of **8Ni** bluish green solid (82%). HRMS ESI m/z: calculated for $C_{104}H_{120}NiN_8O_{32}$ — 2051.7389, found — 2051.7342. ^{1}H NMR (600 MHz, $CDCl_3$) δ, ppm: 8.18 (s, 1H, α-H_{Ar}), 6.75–6.84 (m, 2H, β,γ-H_{Ar}), 4.65–4.72 (bs, 2H, CH_2), 4.23–4.32 (bs, 2H, CH_2), 4.14–4.21 (m, 2H, CH_2), 4.05–4.10 (m, 2H, CH_2), 3.96–4.02 (m, 4H, CH_2). UV-vis ($CHCl_3$), λ, nm (log(ε))*:* 668 (5.22), 604 (4.49), 407 (4.46), 310 (4.83), 286 (4.90).

***Preparation of Co*[(B24C8)$_4$*Pc*] (8*Co*).** A mixture of **8H2** (30 mg, 15 μmol), $Co(OAc)_2$ (5 mg, 30 μmol), and DBU (5 μl, 15 μmol) in 10 mL of DMF was refluxed for 30 min under argon. The reaction mixture was cooled to room temperature and poured into water. The resulting precipitate was filtered, washed with water and dissolved in $CHCl_3$. The solvent was evaporated under vacuum. The product was purified by size-exclusion chromatography (Bio-Beads SX-1 in $CHCl_3$ + 2.5 vol % MeOH) to yield 24 mg of **8Co** as a bluish green solid (78%). HRMS ESI m/z: calculated for $C_{104}H_{120}CoN_8O_{32}$ — 2052.7368, found — 2052.7366. found — 2052.7. ^{1}H NMR (600 MHz, $CDCl_3$) δ, ppm: 10.66 (s, 1H, α-H_{Ar}, 6.78–6.87 (bs, 2H, β,γ-H_{Ar}), 4.98–5.07 (bs, 2H, CH_2), 4.54–4.62 (bs, 2H, CH_2), 4.23–4.31 (m, 4H, CH_2), 4.05–4.17 (m, 4H, CH_2). UV-vis ($CHCl_3$), λ, nm (log(ε))*:* 670 (5.06), 606 (4.49), 402 (4.33), 298 (4.87).

***Preparation of Cu*[(B24C8)$_4$*Pc*] (8*Cu*).** Phthalocyanine **8H2** (48 mg, 24 μmol), was dissolved in 8 mL of DMF and heated to reflux under argon, then $Cu(OAc)_2 \cdot 2H_2O$ (22 mg, 98 μmol) was added in two portions and the mixture was refluxed for 105 min.

The reaction mixture was cooled to room temperature and poured into water. The resulting precipitate was filtered, washed with water and dissolved in $CHCl_3$. The solvent was evaporated under vacuum. Column chromatography on alumina in a CH_2Cl_2/MeOH (95:5) mixture afforded a green compound which was further purified by repetitive size-exclusion chromatography (Bio-Beads SX-1 in $CHCl_3$ + 2.5 vol % MeOH). Yield: 36 mg (72%). HRMS ESI, m/z: calculated for $C_{104}H_{120}CoN_8O_{32}$ — 2057.7332, found — 2057.7302. UV-vis ($CHCl_3$), λ, nm (log(ε)): 678 (5.26), 611 (4.51), 412 (4.46), 341 (4.84).

RESULTS AND DISCUSSION

Synthesis and characterization

The benzo-24-crown-8-phthalonitrile — precursor **7** [37] of the target phthalocyanines — was synthesized by a modified six-step method as shown in Scheme 1. Instead of the previously described tosylation of **4**, iodination was carried out to give compound **5** in moderate yield. In addition, use of a Pd-catalyzed cyanation in the last step instead of a classical Rosenmund–Braun reaction increased the yield of **6** from 55 to 91% [37].

The target metal complexes were synthesized using a template approach (**8Mg** and **8Zn**) or by metalation of free-base phthalocyanine **8H2** with the corresponding metal salts (**8Co**, **8Cu** or **8Ni**) (Scheme 1). Thus, complex **8Mg** was obtained by template condensation of phthalonitrile **7** with $Mg(OAc)_2$ in the presence of DBU with a quite low, 39%, yield. Interestingly, the replacement of $Mg(OAc)_2$ and DBU with metallic Mg in the template reaction increased the yield up to 64%. Using the template method for the synthesis of the previously described **8Zn** afforded this product with a 2.6 times higher yield (87%) than by using the two-step procedure (synthesis of free base ligand **8H2** and its metalation, 33%) [22].

Phthalocyanine **8H2** was obtained by demetallation of **8Mg** with trifluoroacetic acid. This two-step synthesis of

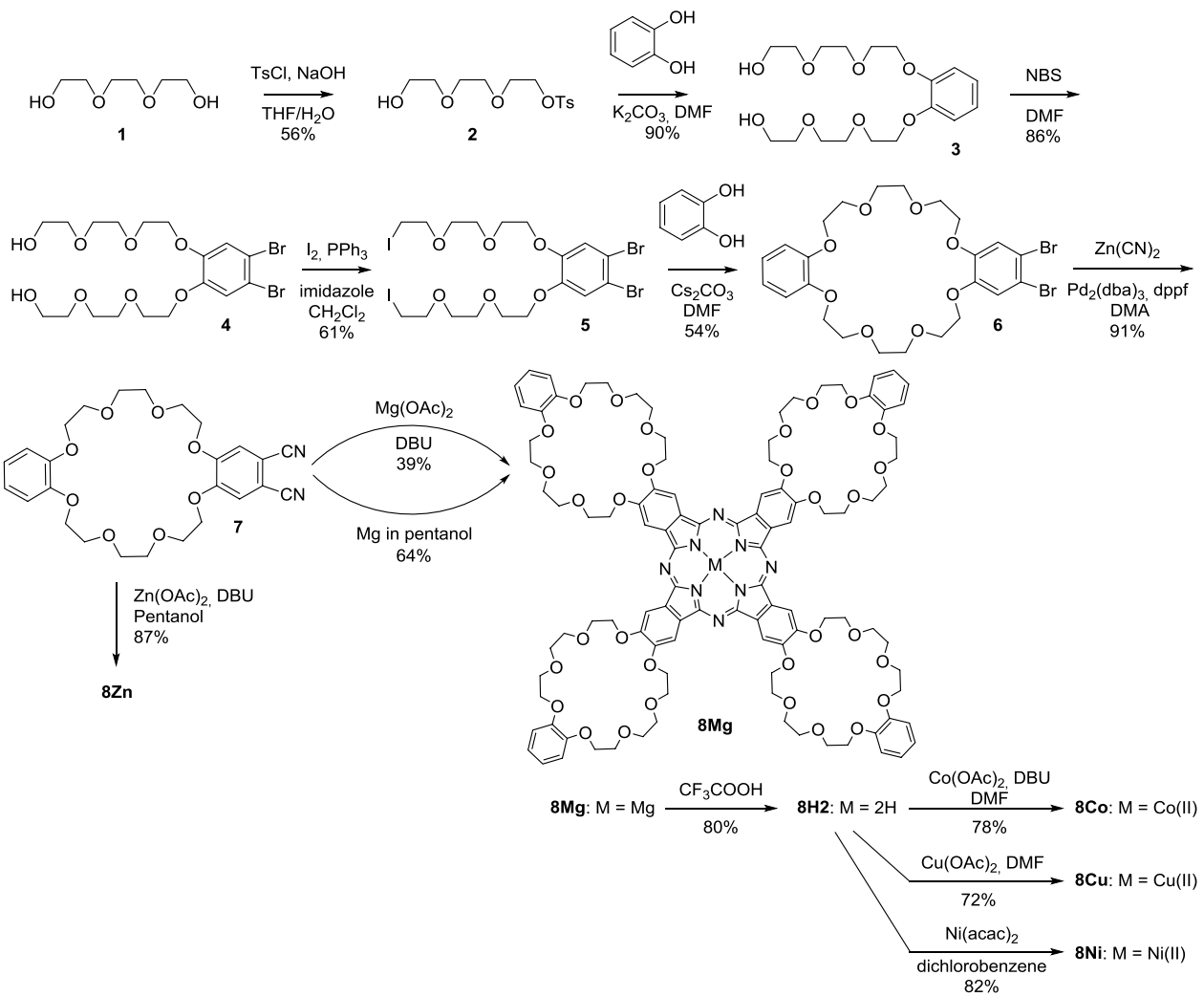

Scheme 1. Synthesis of di-(benzo-24-crown-8)-phthalonitrile **7** and tetra-(benzo-24-crown-8)-phthalocyanines **8M** (**M=Mg(II), Zn(II), Co(II), Cu(II), Ni(II), H2**).

8H2 in 51% yield appeared to be more efficient than the previously described synthesis, with a reported yield of 34% starting from phthalonitrile [21]. Complexes **8Co**, **8Ni** and **8Cu** were synthesized from phthalocyanine **8H2** by metalation with the corresponding metal salts and were isolated with reasonably high yields (78, 82 and 72%, respectively). The metalated compounds were purified by column chromatography on alumina followed by repetitive size-exclusion chromatography on columns packed with Bio-Beads SX-1. All products were characterized by NMR (Fig. 2, Figs S1–S10 in the Supporting information), UV-vis (Fig. 3, Figs S11–S14), HR ESI MS (Figs S15–S20), and EPR (Figs 4–6) spectroscopies.

The molecular structure of the **8Ni** complex was confirmed by its ^{1}H NMR spectrum in $CDCl_3$ which shows two resonance signals of aromatic protons at 8.27 and 6.75–7.84 ppm and five signals of crown ether protons in the aliphatic region of 3.80–4.80 ppm (Fig. 2). The ^{1}H NMR spectra of **8H2** and **8Zn** (Figs S8–S10) are similar, with the same set of the signals. In contrast, the spectrum of complex **8Mg** consists of broad signals that suggest aggregation processes in solution. Surprisingly, despite the paramagnetic nature of the Co(II) nucleus of **8Co**, it was possible to obtain an informative ^{1}H NMR spectrum which displayed a broad signal at low field centered at 10.64 ppm for the phthalocyanine aromatic protons and four sets of signals for the crown ether protons (Fig. 2).

UV-vis properties

The UV-vis spectrum of **8H2** in $CHCl_3$ at $c \approx 10^{-5}$ M displays two intense Q bands at 663 and 701 nm followed by a well-resolved vibrational satellite at 601 nm and a B band at 348 nm that are typical for monomeric phthalocyanines (Fig. 3, Figs S11–S14, Table 1) [38]. The broad band at 420 nm corresponds to a charge transfer band from lone pairs of oxygen atoms to the phthalocyanine aromatic system [39]. Due to the higher symmetry of the metal complexes, only one Q band, in the 668–681 nm region, is observed in the spectra of **8M** solutions, as shown for **8Ni** in Fig. 3.

EPR investigations

Due to the paramagnetic nature of the Co(II) and Cu(II) complexes, **8Co** and **8Cu** were also characterized by EPR spectroscopy. The spectrum of complex **8Cu** was recorded in frozen CH_2Cl_2 at 90 K. Pyridine was added to the solution to prevent aggregation. The spectrum displays hyperfine interaction of spin $S = 1/2$ with the nuclear spin of copper $I = 3/2$ and super hyperfine interaction with four equivalent nitrogen nuclei $I_N = 1$ (Fig. 4). The parameters ($g_z = 2.152$, $g_x = 2.033$, $g_y = 2.037$, $A = 1.932 \times 10^{-2}$ cm^{-1}, $B = 2.067 \times 10^{-3}$ cm^{-1}, $C = 2.011 \times 10^{-3}$ cm^{-1}, a_z(Pc) = 14.82 Gs, a_x(Pc) = 16.33 Gs, a_y (Pc) = 16.96 Gs) are typical for species of this type (Fig. 3) [40,41].

The EPR spectrum of **8Co** in $CHCl_3$ (Fig. 5) reveals hyperfine structure from interaction of spin $S = 1/2$ with the nuclear spin of cobalt $I = 7/2$ with parameters: $g_z = 1.990$, $g_x = 2.352$, $g_y = 2.410$, $A = 1.156 \times 10^{-2}$ cm^{-1}, $B = 5.325 \times 10^{-3}$ cm^{-1}, $C = 8.168 \times 10^{-3}$ cm^{-1}. It is very important to mention that 4.8% of **8Co** is coordinated to O_2. The parameters for the **8Co-O$_2$** complex are: $g_z = 1.985$, $g_x = 1.995$, $g_y = 2.058$, $A = 1.007 \times 10^{-3}$ cm^{-1},

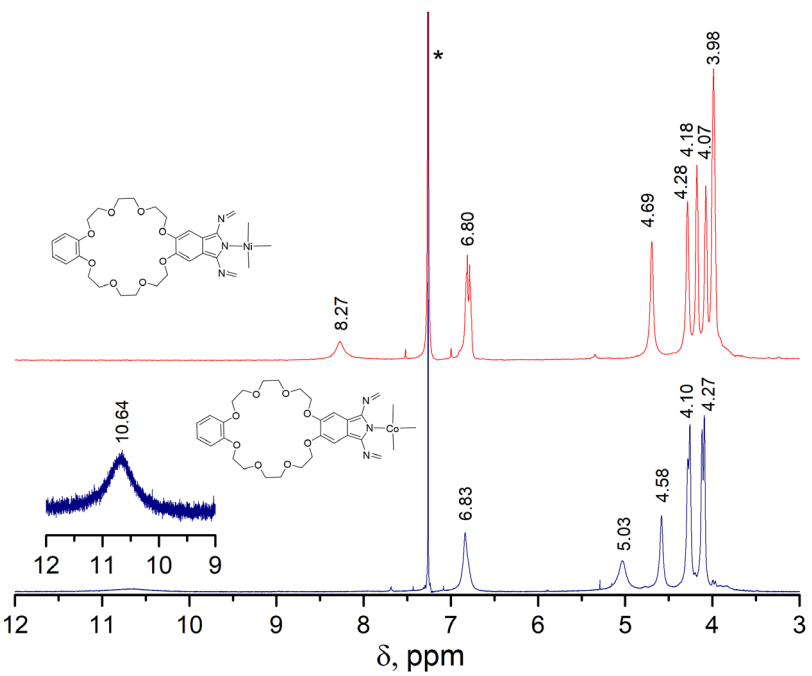

Fig. 2. ^{1}H-NMR spectra of **8Ni** (top) and **8Co** (bottom) in $CDCl_3$.

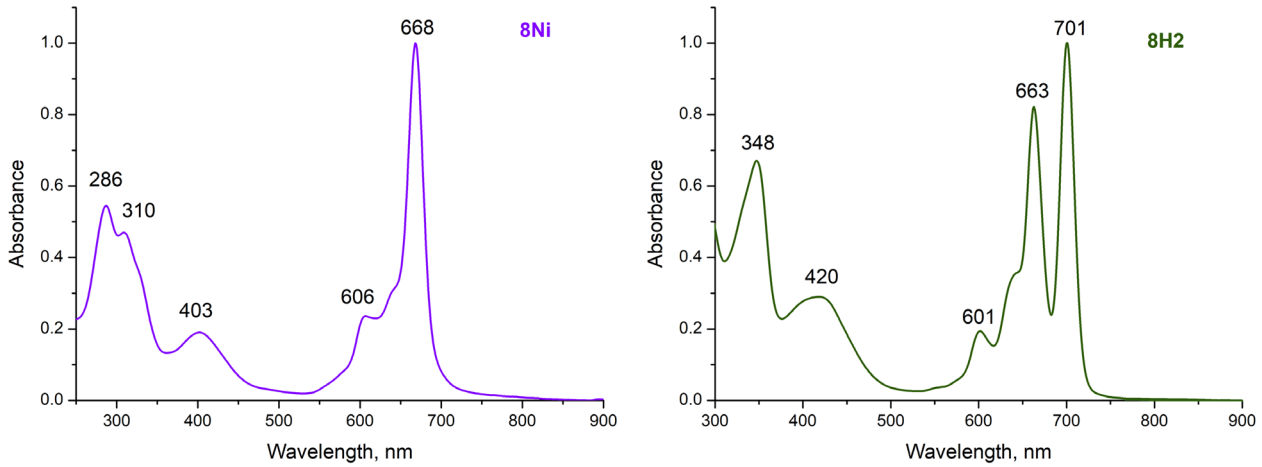

Fig. 3. Normalized UV-vis spectra of **8Ni** (left) and **8H2** (right) in $CHCl_3$.

Table 1. The wavelengths of the Q and B bands of **8M** in the UV-vis spectra in $CHCl_3$.

	8H2	8Mg	8Zn	8Ni	8Co	8Cu
Q-band, nm (log(ε))	663 (5.02), 701 (5.10)	678 (5.30)	680 (5.14)	668 (5.22)	670 (5.06)	678 (5.26)
B-band, nm (log(ε))	348 (4.90)	283 (5.08), 360 (4.92)	358 (4.24)	286 (4.90), 310 (4.83)	298 (4.87)	341 (4.84)

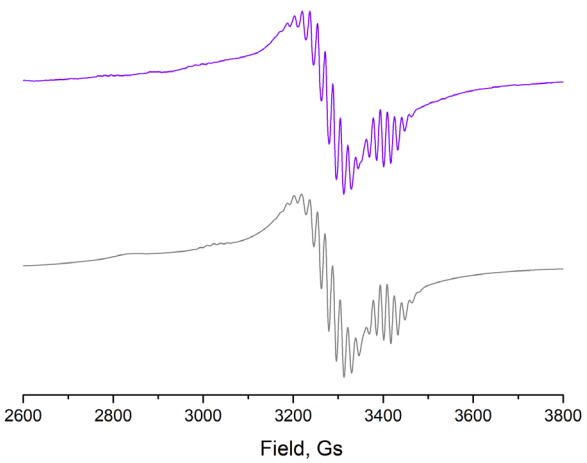

Fig. 4. EPR spectra of **8Cu** in CH_2Cl_2-pyridine (9:1) at 90 K: experimental (violet) and theoretical (grey).

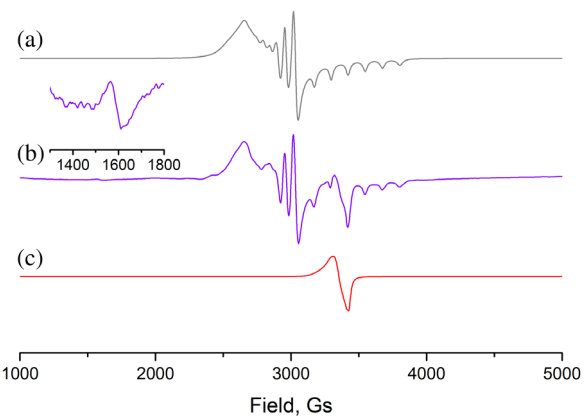

Fig. 5. EPR spectrum of **8Co** in $CHCl_3$ at 90 K (b) and theoretical spectra of **8Co** (a) and **8Co-O$_2$** (c).

$B = 1.694 \times 10^{-3}$ cm^{-1}, $C = 2.344 \times 10^{-3}$ cm^{-1}. In addition, the observation of a prohibited transition signal in the spectrum of **8Co** in $CHCl_3$ at 1600 Gs provided evidence for partial aggregation of the complex.

Addition of pyridine to the **8Co** solution led to significant changes in the EPR spectrum (Fig. 6). The disappearance of the signal at 1600 Gs signified the suppression of the aggregation process. On the other hand, super hyperfine interactions with the coordinated pyridine nitrogen nucleus $I_N = 1$ appeared. The amount of **8Co-O$_2$** complex in the mixture increased more than 10 times — up to 53.9%. This increase is similar to results described earlier for cobalt(II) phthalocyanine [34]. New parameters for monomeric **8Co** are $g_z = 2.003$, $g_x = 2.229$, $g_y = 2.216$, $A = 9.690 \times 10^{-3}$cm^{-1}, $B = 2.390 \times 10^{-3}$ cm^{-1}, $C = 2.400 \times 10^{-3}$ cm^{-1}, a_z(Pyr) = 17.40 Gs, a_x(Pyr) = 6.99 Gs, a_y (Pyr) = 7.75 Gs and for **8Co-O$_2$** complex, the parameters are $g_z = 1.999$, $g_x = 2.009$, $g_y = 2.061$, $A = 1.053 \times 10^{-3}$ cm^{-1}, $B = 1.069 \times 10^{-3}$ cm^{-1} and $C = 1.974 \times 10^{-3}$ cm^{-1}.

The host-guest interactions of MPc with viologen

Next, the interaction of tetra-(benzo-24-crown-8)-phthalocyanine and its host–guest complexes with

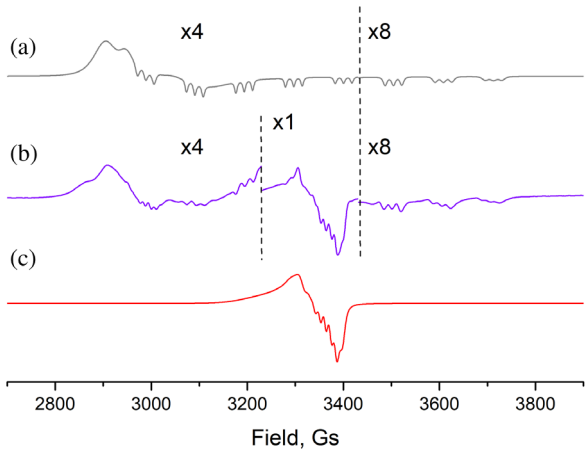

Fig. 6. EPR spectrum of **8Co** in frozen $CHCl_3$-pyridine mixture (4:1) at 90 K (b) and theoretical spectra of **Py-8Co** (a) and **Py-8Co-O$_2$** (c).

viologen **9** (*N*,*N*-dibutynyl-4,4′-bipyridinium) [33] was investigated by UV-vis and EPR spectroscopy. Unfortunately, NMR spectroscopy was not informative, probably due to the presence of several different aggregated forms in solution (Fig. S21).

Complex **8Ni** was chosen as the main object of the supramolecular assembly investigation because of the absence of axial ligands on the central nickel cation that should prevent formation of cofacial dimers. The addition of viologen **9** in acetone or MeCN to a CH_2Cl_2 solution of **8Ni** led to significant hypochromic and hypsochromic shifts (56 nm) of the Q band in the UV-vis spectra, which are typical for the formation of cofacial Pc dimers [40, 42] (Fig. 7 left). Surprisingly, these changes were not observed in the case of $CHCl_3$ solution (Fig. S22); thus, it seems that solvent plays a very important role in the supramolecular aggregation [40]. On the other hand, the solvent in which the viologen was dissolved also plays an important role. Thus, it was demonstrated that acetone was more efficient than acetonitrile for dimerization of Pc (Fig. 7a) probably due to the lower polarity of the acetone compared to acetonitrile. Furthermore, the amount of polar solvent should not be higher than 20% in the final solution. Further increases of the amount of polar solvent led to aggregation of the starting compound and dimerization was not observed. Additionally, increasing the concentration of **8Ni** from 10^{-5} up to 10^{-4} M led to more efficient supramolecular assembly (Fig. S23). The partial aggregation of **8Ni** due to π–π stacking at higher concentration could lead to preorganization of the molecules which would facilitate the formation of cofacial dimers. Dilution studies showed that deviation from the Beer–Lambert–Bouguer law in the spectra of **8Ni** in CH_2Cl_2 solutions starts at concentrations above 10^{-6} (Fig. S24). Unfortunately, the ratio of dimers and monomers in the solution could not be determined from the UV-vis spectra because of overlapping of their low energy absorption bands.

Furthermore, the nature of the central metal cation appeared to play a crucial role in supramolecular processes. Addition of viologen **9** to solutions of **8H2** and **8Cu** led to changes in UV-vis spectra similar to those observed for **8Ni** (Figs S25–26). However, complexes **8Zn**, **8Mg** and **8Co** demonstrated completely different behavior upon addition of viologen. Only minor bathochromic shifts of the Q band were observed, suggesting the formation of other types of supramolecular aggregates (Fig. 7 right, Figs S27–S28). This phenomenon can be explained by the difference in the coordination environment of the central metal atoms. It is well known that cations such as Zn(II), Mg(II) and Co(II) coordinated in a phthalocyanine are able to bind additional axial ligands [43, 44]. EPR studies in this work demonstrated that **8Co** can easily form complexes with axially coordinated O_2. Earlier it was shown that H_2O molecules as an axial ligands on Mg(II) and Zn(II)

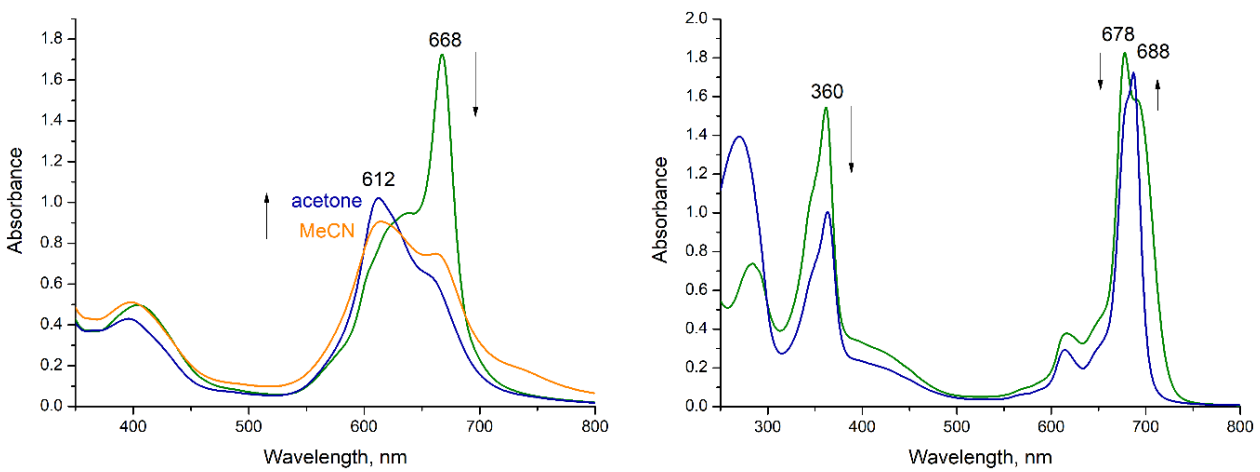

Fig. 7. UV-vis spectra of **8Ni** (left) and **8Mg** (right) in CH_2Cl_2 (c = 10^{-4} M) upon addition of viologen (2 eq.) in MeCN (orange spectrum) or acetone (blue spectra).

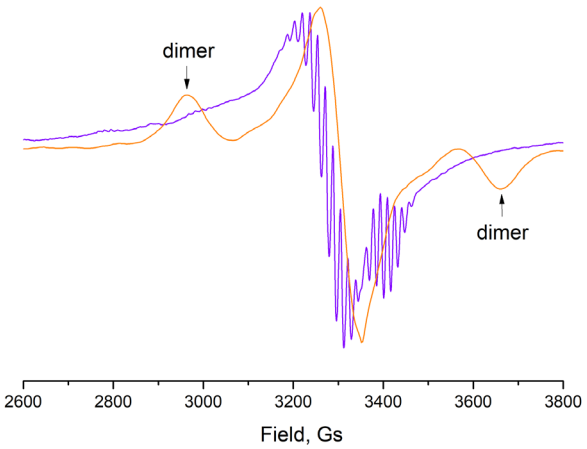

Fig. 8. EPR spectrum of **8Cu** in CH_2Cl_2 (violet) and after addition of viologen **9** (2 eq.) in acetone (orange) at 90 K.

phthalocyanines can sterically hinder the formation of cofacial dimers [43].

Due to the paramagnetic nature of the Cu(II) atom, EPR spectroscopy can be used as an additional method to investigate the supramolecular behavior of **8Cu** in the presence of viologen **9**. The cobalt complex **8Co** was not investigated because the UV-vis study demonstrated that cofacial dimers were not observed upon addition of viologen. The addition of a solution of viologen in acetone to a solution of **8Cu** in CH_2Cl_2 led to the appearance in the EPR spectrum at 90 K of two additional signals with $S = 1$, which are characteristic of a cofacial dimer [45–48] (Fig. 8, Fig. S29). The parameters are: $|D| = 0.0608$ cm^{-1}, $g_z = 2.160$, $g_x = 2.013$, $g_y = 2.013$. The experimental spectrum matches the theoretical one (Fig. S29). Based on the supposition that zero field splitting is caused by dipole–dipole interaction, the Cu–Cu distance can be calculated as R~3.6 Å. The distance between two charged nitrogen atoms in viologen is 7.07 Å, which is noticeably larger, however crown-ethers are conformationally labile, which thus allows the molecules to form dimers. Nevertheless, the signal at H~3300 Gs indicates the presence of the monomeric form of **8Cu** with $S = 1/2$. The ratio of monomer/dimer in the solution is 79/21, but it is important to mention that part of the dimer could be in the $S = 0$ state and, thus, would not be observed in the spectrum.

CONCLUSION

A series of tetra-(benzo-24-crown-8)-substituted phthalocyanines and their Mg(II), Zn(II), Cu(II), Ni(II) and Co(II) complexes were synthesized and characterized by UV-vis absorption, HR, ESI, MS, NMR and EPR spectroscopies. Compounds **8H2**, **8Ni** and **8Cu** form cofacial dimers by supramolecular interactions with viologen molecules in CH_2Cl_2. In contrast, no evidence of cofacial dimers was observed for complexes **8Mg**, **8Zn** and **8Co**, where axial ligands probably prevent this process due to steric hindrance. The important role of solvent and concentration in supramolecular aggregation was also demonstrated. Preorganization of the Pc molecules by π–π stacking seems to be necessary for further supramolecular dimerization. EPR spectroscopy was shown to be efficient in determining the monomer/dimer ratio in assemblies of **8Cu** and viologen **9**. These results could be useful for further application of tetra-(benzo-24-crown-8)-substituted phthalocyanines as a platform in the design of a supramolecular devices and switches.

Acknowledgments

The authors are grateful to the Russian Science Foundation (Grant #18-73-00249). Measurements were performed using equipment of CKP FMI IPCE RAS and IGIC RAS. JAW and JW gratefully acknowledge the CNRS and the University of Strasbourg for financial support.

Supporting information

Figures S1–S29, including spectral data, are given in the supplementary material. This material is available free of charge *via* the Internet at http://www.worldscinet.com/jpp/jpp.shtml.

REFERENCES

1. Sauvage J-P. *Angew. Chemie, Int. Ed.* 2017; **56**: 11080–11093.
2. Cheng C and Stoddart JF. *ChemPhysChem* 2016: 1780–1793.
3. Baroncini M, Casimiro L, de Vet C, Groppi J, Silvi S and Credi A. *ChemistryOpen* 2018; **7**: 169–179.
4. Martynov AG, Safonova EA, Tsivadze AY and Gorbunova YG. *Coord. Chem. Rev.* 2019; **387**: 325–347.
5. Kay ER and Leigh DA. *Angew. Chemie, Int. Ed.* 2015; **54**: 10080–10088.
6. Moulin E, Faour L, Carmona-Vargas CC and Giuseppone N. *Adv. Mater.* 2019; **32**: 1906036.
7. Lerch MM, Hansen MJ, van Dam GM, Szymanski W and Feringa BL. *Angew. Chemie, Int. Ed.* 2016; **55**: 10978–10999.
8. Ambrogio MW, Thomas CR, Zhao YL, Zink JI and Stoddart JF. *Acc. Chem. Res.* 2011; **44**: 903–913.
9. Balzani V, Semeraro M, Venturi M and Credi A. In *Molecular Switches*. Weinheim, Germany: Wiley-VCH Verlag GmbH & Co. KGaA, 2011; 595–627.
10. Green JE, Wook Choi J, Boukai A, Bunimovich Y, Johnston-Halperin E, DeIonno E, Luo Y, Sheriff BA, Xu K, Shik Shin Y, Tseng H-R, Stoddart JF and Heath JR. *Nature* 2007; **445**: 414–417.
11. Kassem S, Lee ATL, Leigh DA, Markevicius A and Solà J. *Nat. Chem.* 2016; **8**: 138–143.

12. Meshkov IN, Bulach V, Gorbunova YG, Kyritsakas N, Grigoriev MS, Tsivadze AY and Hosseini MW. *Inorg. Chem.* 2016; **55**: 10774–10782.
13. Faiz JA, Heitz V and Sauvage J-P. *Chem. Soc. Rev.* 2009; **38**: 422–442.
14. Coutrot F. *ChemistryOpen* 2015; **4**: 556–576.
15. Balzani V, Gómez-López M and Stoddart JF. *Acc. Chem. Res.* 1998; **31**: 405–414.
16. Braunschweig AB, Ronconi CM, Han J-Y, Aricó F, Cantrill SJ, Stoddart JF, Khan SI, White AJP and Williams DJ. *European J. Org. Chem.* 2006; **2006**: 1857–1866.
17. Huang F, Gantzel P, Nagvekar DS, Rheingold AL and Gibson HW. *Tetrahedron Lett.* 2006; **47**: 7841–7844.
18. Koray AR, Ahsen V and Bekâroğlu Ö. *J. Chem. Soc., Chem. Commun.* 1986: 932–933.
19. Yang C, He R, Sun Q, Chen Y and Jiang J. *J. Porphyr. Phthalocyanines* 2019; **23**: 507–517.
20. Martynov AG, Gorbunova YG and Tsivadze AY. *Russ. J. Inorg. Chem.* 2014; **59**: 1635–1664.
21. Yamada Y, Okamoto M, Furukawa K, Kato T and Tanaka K. *Angew. Chemie, Int. Ed.* 2012; **51**: 709–713.
22. Yamada Y, Mihara N and Tanaka K. *Dalton Trans.* 2013; **42**: 15873–15876.
23. Mihara N, Yamada Y and Tanaka K. *Bull. Chem. Soc. Jpn.* 2017; **90**: 427–435.
24. Mihara N, Yamada Y, Takaya H, Kitagawa Y, Aoyama S, Igawa K, Tomooka K and Tanaka K. *Chem. — Eur. J.* 2017; **23**: 7508–7514.
25. Yamada Y, Mihara N, Shibano S, Sugimoto K and Tanaka K. *J. Am. Chem. Soc.* 2013; **135**: 11505–11508.
26. Yamada Y, Kato T and Tanaka K. *Chem. — Eur. J.* 2016; **22**: 12371-12380.
27. Yamada Y, Itoh R, Ogino S, Kato T and Tanaka K. *Angew. Chemie, Int. Ed.* 2017; **56**: 14124–14129.
28. Le Poul N and Colasson B. *ChemElectroChem* 2015; **2**: 475–496.
29. Berville M, Karmazin L, Wytko JA and Weiss J. *Chem. Commun.* 2015; **51**: 15772–15775.
30. Berville M, Choua S, Gourlaouen C, Boudon C, Ruhlmann L, Bailly C, Cobo S, Saint-Aman E, Wytko J and Weiss J. *ChemPhysChem* 2017; **18**: 796–803.
31. Wu L, He Y-M and Fan Q-H. *Adv. Synth. Catal.* 2011; **353**: 2915–2919.
32. Zhou Y, Chen Y, Zhu P-P, Si W, Hou J-L and Liu Y. *Chem. Commun.* 2017; **53**: 3681–3684.
33. Coskun A, Saha S, Aprahamian I and Stoddart JF. *Org. Lett.* 2008; **10**: 3187–3190.
34. Rakitin YV, Larin GM and Minin V V. Interpretation of ESR Spectra of Coordination Compounds (in Russian). Moscow: Nauka; 1993.
35. Lebedev YS and Muromtsev VI. ESR and Relaxation of Stabilized Radicals (in Russian). Moscow: Khimiya; 1972.
36. Wilson R and Kivelson D. *J. Chem. Phys.* 1966; **44**: 154–168.
37. Martínez-Díaz MV, Fender NS, Rodríguez-Morgade MS, Gómez-López M, Diederich F, Echegoyen L, Stoddart JF and Torres T. *J. Mater. Chem.* 2002; **12**: 2095–2099.
38. Fukuda T and Kobayashi N. In *Handbook of Porphyrin Science*. World Scientific: Singapore, 2010; Vol. 9, pp. 1–644
39. Belosludov RV, Nevonen D, Rhoda HM, Sabin JR and Nemykin VN. *J. Phys. Chem. A* 2019; **123**: 132–152.
40. Kobayashi N and Lever ABP. *J. Am. Chem. Soc.* 1987; **109**: 7433–7441.
41. Finazzo C, Calle C, Stoll S, Van Doorslaer S and Schweiger A. *Phys. Chem. Chem. Phys.* 2006; **8**: 1942–1953.
42. Martynov AG, Nefedova I V, Efimov NN, Ugolkova EA, Minin VV, Gorbunova YG and Tsivadze AY. *Macroheterocycles* 2018; **11**: 390–395.
43. Safonova EA, Martynov AG, Nefedov SE, Kirakosyan GA, Gorbunova YG and Tsivadze AY. *Inorg. Chem.* 2016; **55**: 2450–2459.
44. Kramer WW and McCrory CCL. *Chem. Sci.* 2016; **7**: 2506–2515.
45. Smith TD and Pilbrow JR. *Coord. Chem. Rev.* 1974; **13**: 173–278.
46. Kottis P and Lefebvre R. *J. Chem. Phys.* 1963; **39**: 393–403.
47. Thomson C. *Q. Rev. Chem. Soc.* 1968; **22**: 45–74.
48. Eaton SS, More KM, Sawant BM, Boymel PM and Eaton GR. *J. Magn. Reson.* 1983; **52**: 435–449.

